

UNIVERSIDAD DE CONCEPCIÓN



CENTRO DE INVESTIGACIÓN EN
INGENIERÍA MATEMÁTICA (CI²MA)



Numerical solution of an axisymmetric eddy current model with
current and voltage excitations

ALFREDO BERMÚDEZ, BIBIANA LÓPEZ-RODRÍGUEZ,
FRANCISCO JOSÉ PENA, RODOLFO RODRÍGUEZ,
PILAR SALGADO, PABLO VENEGAS

PREPRINT 2021-18

SERIE DE PRE-PUBLICACIONES

Numerical solution of an axisymmetric eddy current model with current and voltage excitations

A. Bermúdez · B. López-Rodríguez ·
F. J. Pena · R. Rodríguez · P. Salgado ·
P. Venegas.

Received: date / Accepted: date

Abstract The aim of this paper is to study the numerical approximation of an axisymmetric time-harmonic eddy current problem involving an in-plane current. The analysis of the problem restricts to the conductor. The source of the problem is given in terms of boundary data currents and/or voltage drops defined in the so-called electric ports, which are parts of the boundary connected to exterior sources. This leads to an elliptic problem written in terms of the magnetic field with nonlocal boundary conditions. First, we prove the existence and uniqueness of the solution for a weak formulation written in terms of Sobolev spaces with appropriate weights. We show that the magnetic field is not the most appropriate variable to impose the boundary conditions when Lagrangian finite elements are used to discretize the problem. We propose an alternative weak formulation of the problem which allows us to avoid this drawback. We compute the numerical solution of the problem by using Lagrangian finite elements ad hoc modified on the vicinity of the symmetry axis. We provide a convergence result under rather general conditions. Moreover, we prove quasi-optimal order error estimates under additional regularity assumptions. Finally, we report numerical results which allow us to confirm the theoretical estimates and to assess the performance of the proposed method in a physical application which is the motivation of this paper: the computation of

A. Bermúdez · F. J. Pena · P. Salgado
Departamento de Matemática Aplicada, Instituto de Matemáticas (IMAT) and
Instituto Tecnológico de Matemática Industrial, Universidade de Santiago de Compostela,
Santiago de Compostela, Spain
E-mail: alfredo.bermudez@usc.es, fran.pena@usc.es, mpilar.salgado@usc.es

B. López-Rodríguez
Escuela de Matemáticas, Universidad Nacional de Colombia, Sede Medellín, Colombia
E-mail: blopezr@unal.edu.co

R. Rodríguez
CI²MA, Departamento de Ingeniería Matemática, Universidad de Concepción, Concepción,
Chile
E-mail: rodolfo@ing-mat.udec.cl

P. Venegas
GIMNAP, Departamento de Matemática, Universidad del Bío-Bío, Concepción, Chile
E-mail: pvenegas@ubiobio.cl

the current density distribution in a steel cylindrical bar submitted to electric-upsetting.

Keywords Axisymmetric problem · eddy-current model · finite elements · error estimates

Mathematics Subject Classification (2020) MSC 65N30 · 78A55 · 78M10

1 Introduction

This paper deals with modeling, mathematical analysis and numerical computation of an axisymmetric eddy current problem characterized by the fact that, on each meridional section of a revolution domain, the current density \mathbf{J} lies in this section; namely, vector \mathbf{J} is of the form $\mathbf{J} := J_r \mathbf{e}_r + J_z \mathbf{e}_z$, being \mathbf{e}_r and \mathbf{e}_z the basis vectors corresponding to radial and axial directions in a cylindrical coordinate system.

This kind of problem arises in several industrial applications where an alternating current passes through a cylindrical workpiece in contact with some parts of another piece connected to an external source. We refer the reader to [2] for a metallurgical application related to electrodes that carry the current into submerged arc furnaces; see also [3] for an application related with circular magnetization in the framework of magnetic particle inspection.

In particular, this paper is motivated by the study of the electromagnetic behavior of a steel bar submitted to a preforming process called electro-upsetting. This process, which actually requires a multiphysics model [20,21], consists in passing a current through a cylindrical bar which is heated by Joule effect and then to deform it to a particular shape; see, for instance Fig. 1. If the current source is alternating, the computation of the current distribution in the cylindrical bar requires the solution of an eddy current model, which can be solved in a meridional section in terms of a current density that has no azimuthal component. The current source is usually given in terms of either the total current at some electric ports of the electro-upsetter connected to a transformer or the voltage drops between such ports. Thus, the typical configuration is the one presented in Fig. 2.

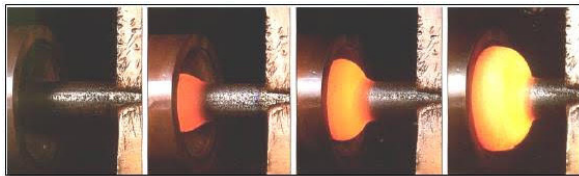


Fig. 1 Enlarging the diameter at the end of a steel bar submitted to electro-upsetting.

The axisymmetric eddy current model with azimuthal current density (or *out of plane current*) has been extensively studied in the literature from modeling, mathematical and numerical points of view; see, for instance, [5], [24], [11], [8], [16] and [14]. This problem has a great interest as it governs the electromagnetic behavior in many applications related to induction heating of cylindrical pieces.

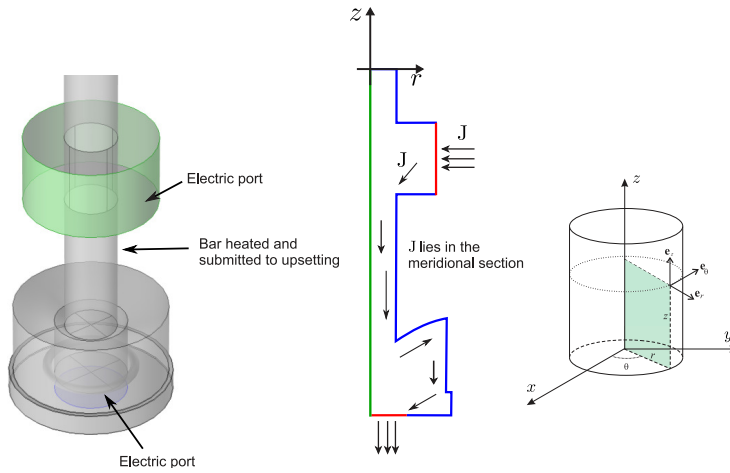


Fig. 2 Sketch of the axisymmetric setting in an electro-upsetting process. The current density lies in a meridional section.

In this case, the most popular and computationally efficient formulation is the one based on the azimuthal component of the magnetic vector potential and this is the classical option implemented in commercial software. However, the mathematical and numerical analysis of the eddy current model involving an *in-plane current*, which is the topic in this paper, has only been covered in a few papers and it offers interesting challenges.

An interesting feature of the axisymmetric problem with an in-plane current is that it can be written in terms of the azimuthal component of the magnetic field and so it can be formulated in the conducting domain by defining suitable boundary conditions without the need of considering air around. This advantage has been exploited from the modeling point of view in a time-harmonic linear case in [2] and in a transient non-linear case in [3]. Concerning the theoretical analysis of these models we refer the reader to [7] which deals with the mathematical analysis of the linear time-harmonic model in the framework of a coupled thermoelectrical analysis and to [4] where the authors address the mathematical and numerical analysis in a transient non-linear case. Both publications consider Dirichlet boundary conditions defined from the total current intensity crossing the domain.

In this paper, we will focus on an axisymmetric formulation of the linear time-harmonic in-plane eddy current model written in terms of the azimuthal component of the magnetic field, H_θ , by considering more general boundary conditions than those cited above [7, 4]. Namely, we will introduce as boundary data currents and/or voltage drops in the electric ports, which are parts of the boundary connected to exterior sources. We refer the reader to [1, Chapter 8] and [5, Chapter 10] for a quite complete review of 3D eddy current problems with electric ports on the boundary. Actually, the model studied in this paper will be similar to that studied in Section 4 from [9] for a 3D conducting domain, but now assuming cylindrical symmetry.

We notice that in order to impose these boundary conditions, a natural unknown for approximating the formulation will be rH_θ instead of H_θ , as in [4]. Although in the continuous problem there is no difference on working with any one of these unknowns as long as suitable weighted Sobolev spaces are chosen in each case, in the discrete case there are remarkable differences. Indeed, the unknown rH_θ offers clear advantages for enforcing exactly the currents and voltage drops which can be imposed by static condensation and by natural source terms in the weak formulation, respectively.

However, using the unknown rH_θ leads to an obvious difficulty when defining and analyzing the discrete schemes, because the term $1/r$ that appears in some integrals introduces singularities at the symmetry axis $r = 0$. We will specially focus on how to deal with these singularities to prove convergence results, in order to be able to provide a theoretical support for a competitive formulation that can be used in many industrial applications. With this aim, we will exploit some techniques introduced recently in [22] for the numerical approximation of an axisymmetric acoustic vibration problem.

We notice that an eddy current formulation in terms of rH_θ can also be found in [6] motivated by the formulation previously introduced in [25]; in these papers, the unknown rH_θ is the natural one to impose non-local source conditions. However, in these references, the axisymmetric domain does not intersect the axis $r = 0$ and currents and voltages on the boundary are not considered. On the other hand, in-plane current problems with current or voltage data have been studied in the continuous case in [24, Section 3.2], but only for two-dimensional non-bounded geometries.

The outline of this paper is as follows: in Section 2 we present the eddy current model in an axisymmetric setting, obtain a formulation in terms of the azimuthal component of the magnetic field and prove that the problem is well posed. We also establish the equivalence between the weak formulations written in terms of H_θ and in terms of rH_θ . In Section 3 we propose a finite element approximation in terms of rH_θ for which we provide a convergence result without assuming any additional regularity of the solution. Then, we prove a quasi-optimal order error estimate in case of having some additional regularity of the continuous solution. In Section 4 we present some numerical experiments that allow us to assess the performance of the proposed method. First, we solve an academic test with known analytical solution to validate the order of convergence provided by the theoretical results. Secondly, we solve an example related to the electric-upsetting, which has been the main motivation of this work. We end the paper with an appendix, where we describe an alternative implementation of the discrete problem based on a mixed formulation that avoids static condensation, which we have used in our numerical tests. The appendix also includes the proof of the equivalence between this mixed problem and the discrete problem previously analyzed.

2 The time-harmonic model in an axisymmetric domain with electric ports

In this section we describe the eddy currents model in an axisymmetric domain with electric ports. We will see that the cylindrical symmetry allows us to state the problem only in the conducting part by using suitable boundary conditions.

Let us assume that $\widehat{\Omega}$ is cylindrically symmetric, namely

$$\widehat{\Omega} := \{(r, \theta, z) : 0 \leq \theta \leq 2\pi, (r, z) \in \Omega\},$$

for some bounded subset $\Omega \subset \mathbb{R}^2$. Let $\mathbf{n} = n_r \mathbf{e}_r + n_z \mathbf{e}_z$ be the outward unit normal vector to $\partial\Omega$; from now on we assume $n_r \geq 0$. Moreover we restrict our attention to a simply connected set $\widehat{\Omega}$ that intersects the axis $r = 0$ at a set of positive one dimensional measure, so that Ω is also simply connected.

Let us further assume that the physical properties, electrical conductivity, σ , and magnetic permeability, μ , are independent on θ , i.e.,

$$\sigma := \sigma(r, z), \quad \mu := \mu(r, z),$$

and that source currents are such that the current density in the conducting part is of the form

$$\mathbf{J}(r, \theta, z) := J_r(r, z) \mathbf{e}_r + J_z(r, z) \mathbf{e}_z$$

and, of course, null in the dielectric.

Under these assumptions it is possible to define an eddy current model restricted to the conducting domain $\widehat{\Omega}$ by using suitable boundary conditions on its boundary. Firstly, we notice that the classical time-harmonic eddy current model restricted to $\widehat{\Omega}$ and to linear magnetic materials leads to find a magnetic field \mathbf{H} and an electric field \mathbf{E} of the form,

$$i\omega \mathbf{B} + \mathbf{curl} \mathbf{E} = \mathbf{0} \quad \text{in } \widehat{\Omega}, \quad (1a)$$

$$\mathbf{curl} \mathbf{H} = \mathbf{J} \quad \text{in } \widehat{\Omega}, \quad (1b)$$

$$\mathbf{div} \mathbf{B} = 0, \quad \text{in } \widehat{\Omega}, \quad (1c)$$

$$\mathbf{B} = \mu \mathbf{H}, \quad (1d)$$

$$\mathbf{J} = \sigma \mathbf{E}, \quad (1e)$$

ω being the angular frequency, i.e., $\omega = 2\pi f$ with f the electric current frequency.

By assuming that none of the fields depend on θ , we can look for a solution of the previous equations satisfying,

$$\mathbf{E}(r, \theta, z) := E_r(r, z) \mathbf{e}_r + E_z(r, z) \mathbf{e}_z,$$

$$\mathbf{H}(r, \theta, z) := H_\theta(r, z) \mathbf{e}_\theta.$$

Consequently, the following boundary condition can be imposed on the whole boundary of the conducting domain:

$$\mu \mathbf{H} \cdot \mathbf{n} = 0 \quad \text{on } \partial\widehat{\Omega} \quad (2)$$

where \mathbf{n} is the outward unit normal to $\partial\widehat{\Omega}$. This property will allow us setting boundary conditions on $\partial\widehat{\Omega}$, in order to impose currents and/or voltage drops on electric ports. Indeed, let assume that the boundary of $\widehat{\Omega}$ splits as follows:

$$\partial\widehat{\Omega} := \widehat{\Gamma}_N \cup \widehat{\Gamma}_J \cup \widehat{\Gamma}_E$$

where $\widehat{\Gamma}_J$ and $\widehat{\Gamma}_E$ are the part of the boundary connected to an electric source with known voltage drops or currents, while $\widehat{\Gamma}_N$ is the isolated part, i.e., there is no current flux through this boundary. In eddy currents models with electric ports it

is usual to assume that currents enter and exit the domain perpendicularly and consequently, we will assume

$$\mathbf{E} \times \mathbf{n} = \mathbf{0} \quad \text{on } \widehat{\Gamma}_J \cup \widehat{\Gamma}_E, \quad (3)$$

while the isolation condition means

$$\mathbf{J} \cdot \mathbf{n} = \mathbf{curl} \mathbf{H} \cdot \mathbf{n} = 0 \quad \text{on } \widehat{\Gamma}_N. \quad (4)$$

From condition (2) we can deduce that there exists a sufficiently smooth function V defined in $\widehat{\Omega}$ up to a constant, such that $V|_{\partial\widehat{\Omega}}$ is a surface potential of the tangential component of \mathbf{E} , namely, $\mathbf{E} \times \mathbf{n} = -\text{grad}V \times \mathbf{n}$ on $\partial\widehat{\Omega}$. On the other hand, (3) implies that V must be constant on each connected component of $\widehat{\Gamma}_J \cup \widehat{\Gamma}_E$ to be called port. We assume that the whole $\widehat{\Gamma}_E$ is a port and denote the ports of $\widehat{\Gamma}_J$ as $\widehat{\Gamma}_J^k$, k being its number. We will assume that $V = 0$ on $\widehat{\Gamma}_E$ and then the complex number $V_k := V|_{\widehat{\Gamma}_J^k} - V|_{\widehat{\Gamma}_E}$ is the voltage drop between $\widehat{\Gamma}_J^k$ and $\widehat{\Gamma}_E$; consequently, $V_k := V|_{\widehat{\Gamma}_J^k}$.

According to the previous discussion, for each surface $\widehat{\Gamma}_J^k$, we will assume that we know

- either voltage drop $V_k := V|_{\widehat{\Gamma}_J^k}$
- or the current intensity going through $\widehat{\Gamma}_J^k$, i.e.,

$$\int_{\widehat{\Gamma}_J^k} \mathbf{J} \cdot \mathbf{n} = \int_{\widehat{\Gamma}_J^k} \mathbf{curl} \mathbf{H} \cdot \mathbf{n} = I_k.$$

To obtain a weak formulation of this problem, let us multiply the Faraday equation defined in $\widehat{\Omega}$ by a smooth test function \mathbf{G} such that $\mathbf{curl} \mathbf{G} \cdot \mathbf{n} = 0$ on $\widehat{\Gamma}_N$. From Ampère and Ohm's laws we obtain

$$\int_{\widehat{\Omega}} i\omega\mu\mathbf{H} \cdot \bar{\mathbf{G}} + \int_{\widehat{\Omega}} \mathbf{E} \cdot \mathbf{curl} \bar{\mathbf{G}} = \int_{\widehat{\Omega}} i\omega\mu\mathbf{H} \cdot \bar{\mathbf{G}} + \int_{\widehat{\Omega}} \frac{1}{\sigma} \mathbf{curl} \mathbf{H} \cdot \mathbf{curl} \bar{\mathbf{G}} = - \int_{\widehat{\Omega}} \text{grad}V \cdot \mathbf{curl} \bar{\mathbf{G}}$$

and using a Green's formula

$$\begin{aligned} & \int_{\widehat{\Omega}} i\omega\mu\mathbf{H} \cdot \bar{\mathbf{G}} + \int_{\widehat{\Omega}} \frac{1}{\sigma} \mathbf{curl} \mathbf{H} \cdot \mathbf{curl} \bar{\mathbf{G}} \\ &= - \int_{\widehat{\Omega}} \text{grad}V \cdot \mathbf{curl} \bar{\mathbf{G}} = - \int_{\partial\widehat{\Omega}} V \mathbf{curl} \bar{\mathbf{G}} \cdot \mathbf{n} = - \int_{\widehat{\Gamma}_J} V \mathbf{curl} \bar{\mathbf{G}} \cdot \mathbf{n} \end{aligned} \quad (5)$$

where in the last equality we have used that $V = 0$ on $\widehat{\Gamma}_E$.

Next, we will rewrite this weak formulation in cylindrical coordinates. Let us denote by $\partial\Omega$ the boundary of Ω which can be decomposed as $\partial\Omega := \Gamma_D \cup \Gamma_J \cup \Gamma_N \cup \Gamma_E$ being Γ_D the symmetry axis $r = 0$.

We will write the above weak formulation for a magnetic field $\mathbf{H}(r, \theta, z) = H_\theta(r, z)\mathbf{e}_\theta$ and test functions of the form $\mathbf{G}(r, \theta, z) = G_\theta(r, z)\mathbf{e}_\theta$.

First of all, we notice that for these functions

$$\mathbf{curl} \mathbf{G} = -\frac{\partial G_\theta}{\partial z} \mathbf{e}_r + \frac{1}{r} \frac{\partial}{\partial r} (rG_\theta) \mathbf{e}_z$$

and hence,

$$\mathbf{curl} \mathbf{G} \cdot \mathbf{n} = -\frac{\partial G_\theta}{\partial z} n_r + \frac{1}{r} \frac{\partial}{\partial r} (r G_\theta) n_z = \frac{1}{r} \frac{\partial (r G_\theta)}{\partial \boldsymbol{\tau}}, \text{ on } \partial\Omega,$$

where $\boldsymbol{\tau}$ is a clockwise unit tangent vector to $\partial\Omega$.

Therefore, the isolated condition $\mathbf{curl} \mathbf{H} \cdot \mathbf{n} = \mathbf{0}$ leads to $\frac{\partial (r H_\theta)}{\partial \boldsymbol{\tau}} = 0$ and then $r H_\theta$ has to be constant on each connected component of $\widehat{\Gamma}_N$. Thus, we consider $\Gamma_N := \bigcup_{k=0}^N \Gamma_N^k$, being Γ_N^k the $N+1$ connected components of Γ_N and let us assume that Γ_N^0 is the one which touches the symmetry axis and is placed between the symmetry axis and a connected component of Γ_J ; see Fig. 3. This assumption is not restrictive in most physical applications.

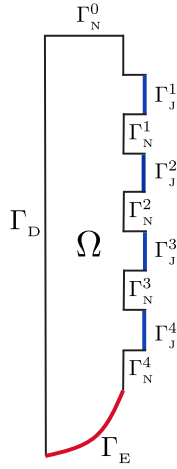


Fig. 3 Representation of the meridian section Ω of the axisymmetric domain $\widehat{\Omega}$.

On the other hand, let us assume that Γ_J also has N connected components and $\Gamma_J := \bigcup_{k=1}^N \Gamma_J^k$. For $k = 1, \dots, N$, we have (see Fig. 3),

$$\begin{aligned} \int_{\widehat{\Gamma}_J^k} \mathbf{curl} \mathbf{H} \cdot \mathbf{n} &= I_k = 2\pi \int_{\Gamma_J^k} \frac{1}{r} \frac{\partial (r H_\theta)}{\partial \boldsymbol{\tau}} r \, dl \\ &= 2\pi \int_{\Gamma_J^k} \frac{\partial (r H_\theta)}{\partial \boldsymbol{\tau}} \, dl = 2\pi (r H_\theta)|_{\Gamma_N^k} - 2\pi (r H_\theta)|_{\Gamma_N^{k-1}}. \end{aligned}$$

Thus, we can write

$$(r H_\theta)|_{\Gamma_N^k} - (r H_\theta)|_{\Gamma_N^{k-1}} = \frac{I_k}{2\pi}, \quad k = 1, \dots, N.$$

Get to this point and as has been advanced before, we will distinguish between ports in Γ_J where we know the currents from those where the voltage drops are

given; namely, the set of indices corresponding to the connected component of Γ_j are divided into two disjoint subsets: $\{1, \dots, N\} = N_I \cup N_V$, where

- For $k \in N_V$, voltage drop $V_k \in \mathbb{C}$ is a given data.
- For $k \in N_I$, current $I_k \in \mathbb{C}$ is a given data.

Consequently, the above 3D weak formulation could be written in terms of H_θ as we detail below. To attain this goal, we introduce some weighted Sobolev spaces that will be used in what follows and establish some of their properties. More general results can be found in [12], [18], [13] and [10]. For $\vartheta \subseteq \Omega$ and $\alpha \in \mathbb{R}$, let $L_\alpha^2(\vartheta)$ be the weighted Lebesgue space of measurable functions G defined in ϑ with bounded norm

$$\|G\|_{L_\alpha^2(\vartheta)}^2 := \int_\vartheta |G|^2 r^\alpha dr dz.$$

Given $k \in \mathbb{N}$, the weighted Sobolev space $H_1^k(\vartheta)$ consists of all functions in $L_1^2(\vartheta)$ whose derivatives in the sense of distributions up to order k are also in $L_1^2(\vartheta)$. We define the norms and semi-norms of these spaces in the standard way; for instance, in $H_1^1(\vartheta)$ the semi-norm

$$|G|_{H_1^1(\vartheta)}^2 := \int_\vartheta \left(|\partial_r G|^2 + |\partial_z G|^2 \right) r dr dz.$$

Throughout the paper, we will use the following Hilbert spaces:

$$\begin{aligned} \tilde{H}_1^1(\vartheta) &:= H_1^1(\vartheta) \cap L_{-1}^2(\vartheta), \\ \tilde{H}_1^2(\vartheta) &:= \left\{ G \in \tilde{H}_1^1(\vartheta) : \|G\|_{\tilde{H}_1^2(\vartheta)} < \infty \right\}, \end{aligned}$$

with their respective norms defined by

$$\|G\|_{\tilde{H}_1^1(\vartheta)}^2 := \|G\|_{H_1^1(\vartheta)}^2 + \|G\|_{L_{-1}^2(\vartheta)}^2, \quad (6)$$

$$\|G\|_{\tilde{H}_1^2(\vartheta)}^2 := \|G\|_{\tilde{H}_1^1(\vartheta)}^2 + \left| r^{-1} \partial_r(rG) \right|_{H_1^1(\vartheta)}^2 + \|\partial_z G\|_{H_1^1(\vartheta)}^2. \quad (7)$$

The following results will be used in the sequel.

Lemma 1 *There holds $H_1^1(\Omega) \hookrightarrow L_{-1+\varepsilon}^2(\Omega)$ continuously for all $\varepsilon > 0$.*

Proof See [18, Remark 4.1].

Lemma 2 *For all $G \in \tilde{H}_1^1(\Omega)$, $\partial_r(rG)$ belongs to $L_{-1}^2(\Omega)$ and satisfies*

$$\|\partial_r G\|_{L_1^2(\Omega)}^2 + \|G\|_{L_{-1}^2(\Omega)}^2 \leq \|\partial_r(rG)\|_{L_{-1}^2(\Omega)}^2 \leq 2\|\partial_r G\|_{L_1^2(\Omega)}^2 + 2\|G\|_{L_{-1}^2(\Omega)}^2.$$

Proof This result is proved in [13, Proposition 3.1] for a square domain. By proceeding as in this reference we write

$$\|\partial_r(rG)\|_{L_{-1}^2(\Omega)}^2 = \|\partial_r G\|_{L_1^2(\Omega)}^2 + \|G\|_{L_{-1}^2(\Omega)}^2 + 2 \int_\Omega G \partial_r G dr dz.$$

By integration by parts, the last term on the right-hand side of the previous equation can be written as follows

$$2 \int_\Omega G \partial_r G dr dz = \int_\Omega \partial_r(G^2) dr dz = \int_{\partial\Omega} G^2 n_r.$$

Since $n_r \geq 0$, the result is a consequence of the previous equalities. \square

In order to establish a weak formulation of (5), we consider the following subspace of $\tilde{\mathbf{H}}_1^1(\Omega)$

$$\mathcal{V} := \left\{ G_\theta \in \tilde{\mathbf{H}}_1^1(\Omega) : (rG_\theta)|_{\Gamma_N^k} = \text{constant} \quad k = 0, \dots, N \right\}.$$

For $\mathbf{I} := (I_k)_{k \in N_I}$ we also define

$$\mathcal{V}(\mathbf{I}) := \left\{ G_\theta \in \mathcal{V} : (rG_\theta)|_{\Gamma_N^0} = 0, (rG_\theta)|_{\Gamma_N^k} = (rG_\theta)|_{\Gamma_N^{k-1}} + \frac{I_k}{2\pi}, k \in N_I \right\}.$$

By using test functions of the form $\mathbf{G} = G_\theta(r, z)\mathbf{e}_\theta$ in (5) we obtain the following weak formulation of the problem in terms of H_θ .

Problem 1 Given $V_k \in \mathbb{C}$ for $k \in N_V$, and $I_k \in \mathbb{C}$ for $k \in N_I$, find $H_\theta \in \mathcal{V}(\mathbf{I})$ such that

$$\begin{aligned} \int_{\Omega} i\omega\mu H_\theta \bar{G}_\theta r dr dz + \int_{\Omega} \frac{1}{\sigma} \left(\frac{\partial H_\theta}{\partial z} \frac{\partial \bar{G}_\theta}{\partial z} + \frac{1}{r^2} \frac{\partial}{\partial r} (rH_\theta) \frac{\partial}{\partial r} (r\bar{G}_\theta) \right) r dr dz \\ = - \sum_{k \in N_V} V_k \left((r\bar{G}_\theta)|_{\hat{\Gamma}_N^k} - (r\bar{G}_\theta)|_{\hat{\Gamma}_N^{k-1}} \right) \quad \forall G_\theta \in \mathcal{V}(\mathbf{0}). \end{aligned}$$

As will be shown below $\mathcal{V}(\mathbf{I}) \neq \emptyset$ (see Corollary 1) then, the well-posedness of this weak formulation can be proved by using Lemma 2 and the Lax-Milgram lemma.

Notice that the constraints included in the functional space introduces difficulties from a numerical point of view. In fact, when a finite element method is used to approximate the previous problem, G_θ is assumed to be piecewise polynomial and thus, the constraint $rG_\theta = \text{constant}$ implies that $G_\theta = 0$. To avoid this drawback we will propose an alternative for its numerical analysis which will be based on reformulating the problem in terms of $\tilde{H} := rH_\theta$. To simplify the notation we drop subscript θ for the new unknown. For this purpose, let us introduce the notation $\tilde{G}^k := \tilde{G}|_{\Gamma_N^k}$, $k = 0, \dots, N$ and the function space

$$\mathcal{X} := \left\{ \tilde{G} \in H_{-1}^1(\Omega) : \tilde{G}^k = \text{constant}, k = 0, \dots, N \right\}.$$

We also introduce the sesquilinear form $a : \mathcal{X} \times \mathcal{X} \rightarrow \mathbb{C}$ given by

$$a(\tilde{H}, \tilde{G}) := \int_{\Omega} \frac{i\omega\mu}{r} \tilde{H} \bar{\tilde{G}} dr dz + \int_{\Omega} \frac{1}{r\sigma} \text{grad} \tilde{H} \cdot \text{grad} \bar{\tilde{G}} dr dz.$$

For $\mathbf{I} := (I_k)_{k \in N_I}$ we define

$$\mathcal{X}(\mathbf{I}) := \left\{ \tilde{G} \in \mathcal{X} : \tilde{G}^0 = 0, \tilde{G}^k = \tilde{G}^{k-1} + \frac{I_k}{2\pi}, k \in N_I \right\}.$$

Using the previous definitions we rewrite Problem 1 in terms of the new variable \tilde{H} as follows:

Problem 2 Given $V_k \in \mathbb{C}$ for $k \in N_V$ and $I_k \in \mathbb{C}$ for $k \in N_I$, find $\tilde{H} \in \mathcal{X}(\mathbf{I})$ such that

$$a(\tilde{H}, \tilde{G}) = - \sum_{k \in N_V} V_k (\bar{\tilde{G}}^k - \bar{\tilde{G}}^{k-1}) \quad \forall \tilde{G} \in \mathcal{X}(\mathbf{0}).$$

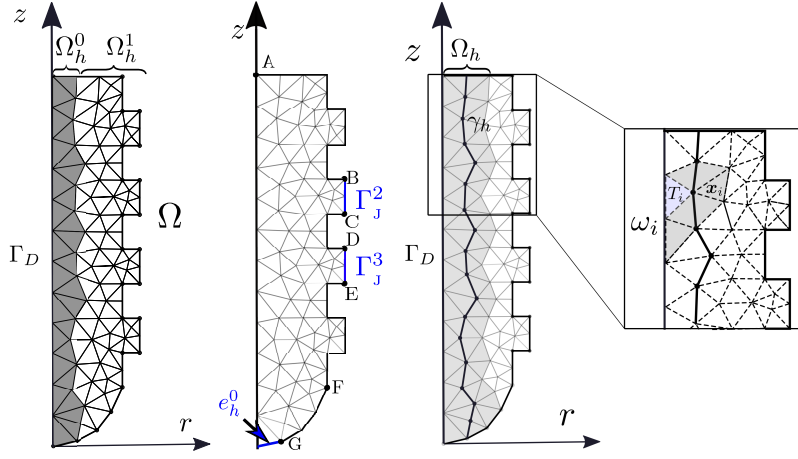


Fig. 4 Decomposition of the finite element triangulation \mathcal{T}_h (left). Notations used in the proof of Lemmas 3 (center) and 5 (right).

The existence and uniqueness of solution of the previous problem follows from the fact that $\mathcal{X}(\mathbf{I})$ is nonempty which will be shown below (see Lemma 3) and the Lax-Milgram lemma. Actually, the well-posedness of Problem 2 can be also derived from the fact that problems 1 and 2 are equivalent in the sense that H_θ is a solution of Problem 1 if and only if rH_θ solves Problem 2, which follows from the following relation: if $G \in \tilde{\mathbf{H}}_1^1(\Omega)$ then $rG \in \mathbf{H}_{-1}^1(\Omega)$. Moreover, (cf. Lemma 2)

$$\|G\|_{\tilde{\mathbf{H}}_1^1(\Omega)}^2 \leq \|rG\|_{\mathbf{H}_{-1}^1(\Omega)}^2 \leq 2\|G\|_{\tilde{\mathbf{H}}_1^1(\Omega)}^2. \quad (8)$$

3 Finite element approximation

In this section we introduce a Galerkin approximation of Problem 2 and prove some convergence results. We assume that $\{\mathcal{T}_h\}_{h>0}$ is a regular family of partitions of $\bar{\Omega}$ in triangles T so that the edges of the triangulation lying on $\partial\Omega$ belong only to Γ_D , Γ_J , Γ_N , or Γ_E ; parameter h stands for the mesh-size and, from now on, we assume that any generic constant denoted by C is independent of h and r . We denote

$$\mathcal{T}_h^0 := \{T \in \mathcal{T}_h : T \cap \Gamma_D \neq \emptyset\}, \quad \mathcal{T}_h^1 = \mathcal{T}_h \setminus \mathcal{T}_h^0$$

and define the open sets $\Omega_h^1, \Omega_h^0 \subset \Omega$ such that $\bar{\Omega}_h^1 := \bigcup_{T \in \mathcal{T}_h^0} T$, and $\bar{\Omega}_h^0 := \bigcup_{T \in \mathcal{T}_h^1} T$ (see Fig. 4 (left)). For any $K \subset \Omega$, we define $r_{\max}^K := \max\{r : (r, z) \in K\}$ and $r_{\min}^K := \min\{r : (r, z) \in K\}$. The following inequalities hold: for all $T \in \mathcal{T}_h^1$,

$$r_{\min}^T \geq Ch_T, \quad r_{\max}^T \leq Cr_{\min}^T. \quad (9)$$

Moreover, clearly, $r_{\max}^T < Ch_T$ for all $T \in \mathcal{T}_h^0$.

Let \mathcal{Y}_h be the space of piecewise linear continuous finite elements with vanishing values in Ω_h^1 ,

$$\mathcal{Y}_h := \{\tilde{G}_h \in \mathcal{C}(\bar{\Omega}) : \tilde{G}_h = 0 \text{ in } \Omega_h^1, \tilde{G}_h|_T \in \mathbb{P}_1(T) \ \forall T \in \mathcal{T}_h^1\} \quad (10)$$

and

$$\mathcal{X}_h := \{\tilde{G}_h \in \mathcal{Y}_h : \tilde{G}_h|_{\Gamma_N^k} = \text{constant}, k = 0, \dots, N\} \subset \mathcal{X}.$$

We use the same notation as in the continuous case and define $\tilde{G}_h^k := \tilde{G}_h|_{\Gamma_N^k}$, $k = 0, \dots, N$. Whence, for $\mathbf{I} = (I_k)_{k \in N_I}$, the natural approximation space of $\mathcal{X}(\mathbf{I})$ is

$$\mathcal{X}_h(\mathbf{I}) := \left\{ \tilde{G}_h \in \mathcal{X}_h : \tilde{G}_h^0 = 0, \tilde{G}_h^k = \tilde{G}_h^{k-1} + \frac{I_k}{2\pi}, k \in N_I \right\}. \quad (11)$$

The Galerkin approximation of Problem 2 reads as follows:

Problem 3 Find $\tilde{H}_h \in \mathcal{X}_h(\mathbf{I})$ such that

$$a(\tilde{H}_h, \tilde{G}_h) = - \sum_{k \in N_V} V_k (\tilde{G}_h^{k-1} - \tilde{G}_h^{k-2}) \quad \forall \tilde{G}_h \in \mathcal{X}_h(\mathbf{0}).$$

The existence and uniqueness of solution to Problem 3 is a consequence of the following lemma.

Lemma 3 Let $\mathbf{I} = (I_k)_{k \in N_I}$, then $\mathcal{X}_h(\mathbf{I}) \neq \emptyset$.

Proof Let e_h^0 be the unique edge of Γ_E intersecting Γ_D (see Fig. 4 (center)) and $\Gamma := \Gamma_N \cup \Gamma_J \cup \Gamma_E$ (see Fig. 3). We define \tilde{G}_Γ , a continuous piecewise linear function in Γ such that:

- $\tilde{G}_\Gamma = 0$ in Γ_N^0 and e_h^0 ,
- \tilde{G}_Γ is constant in Γ_N^k for $k = 1, \dots, N$, and in Γ_J^k , $k \in N_V$,
- \tilde{G}_Γ restricted to each Γ_J^k , $k \in N_I$, is linear and such that the values at the ends of the segment Γ_J^k differ in $\frac{I_k}{2\pi}$.

By extending the aforementioned function to the interior of the domain we obtain an element in $\mathcal{X}_h(\mathbf{I})$. \square

Remark 1 For a better understanding of how to build a function \tilde{G}_Γ in the proof of Lemma 3, we consider the boundary configuration given in Fig. 4 (center), where the construction of \tilde{G}_Γ when $k \in N_I = \{2, 3\}$ is the following: \tilde{G}_Γ vanishes from point A to B and evaluated at point C is equal to $\frac{I_2}{\pi}$. From point C to D it is constant and evaluated at point E is equal to $\frac{I_2 + I_3}{2\pi}$. Finally, from point E to F, the function \tilde{G}_Γ is constant and from F to G it is piecewise linear continuous and vanishes at G.

As an immediate consequence of the previous result we have

Corollary 1 Let $\mathbf{I} = (I_k)_{k \in N_I}$ and $\tilde{G}_h \in \mathcal{X}_h(\mathbf{I})$ be defined as in the previous lemma. Since \tilde{G}_h vanishes in Ω_h^1 , then \tilde{G}_h/r is well defined and belongs to $\mathcal{V}(\mathbf{I})$.

3.1 Convergence

In this section we prove that the Galerkin approximation given by Problem 3 converges to the solution of Problem 2. We obtain a convergence result in the H_{-1}^1 -norm without assuming any additional regularity of the solution. Moreover, under appropriate smoothness assumptions, we also obtain a quasi-optimal-order error estimate.

To begin with we introduce the classical Scott-Zhang operator $I_h : H^1(\Omega) \rightarrow \mathcal{L}_h$, where the finite element space \mathcal{L}_h is defined by:

$$\mathcal{L}_h := \{ \psi_h \in \mathcal{C}(\overline{\Omega}) : \psi_h|_T \in \mathbb{P}_1(T) \quad \forall T \in \mathcal{T}_h \}.$$

Let us recall that this operator preserves piecewise linear values at the boundary (see [23]). We also introduce $\tilde{I}_h : H^1(\Omega) \cap H_{-1}^1(\Omega) \rightarrow \mathcal{Y}_h$ such that $\tilde{I}_h \tilde{G}$ is defined differently in the triangles in \mathcal{T}_h^0 and \mathcal{T}_h^1 . On the former, we just define $\tilde{I}_h \tilde{G} = 0$. On the latter, $\tilde{I}_h \tilde{G}$ is $I_h \tilde{G}$, the classical Scott-Zhang interpolant of \tilde{G} , connected such that the resulting interpolant $\tilde{I}_h \tilde{G} \in \mathcal{C}(\overline{\Omega})$. Namely, on those triangles $T \in \mathcal{T}_h^1$ with a vertex \mathbf{x} on $\gamma_h := \partial\Omega_h^1 \cap \partial\Omega_h^1$ (see Fig. 4 (right)) we consider $\tilde{I}_h \tilde{G}(\mathbf{x}) = 0$.

For any $T \in \mathcal{T}_h$, let ω_T be the union of all triangles that intersect triangle T . It is well known that, for all $\tilde{G} \in H^1(\omega_T)$,

$$\|\tilde{G} - I_h \tilde{G}\|_{L^2(T)} + h|\tilde{G} - I_h \tilde{G}|_{H^1(T)} \leq Ch|\tilde{G}|_{H^1(\omega_T)} \quad (12)$$

and, for all $\tilde{G} \in H^2(\omega_T)$,

$$|\tilde{G} - I_h \tilde{G}|_{H^1(T)} \leq Ch|\tilde{G}|_{H^2(\omega_T)}. \quad (13)$$

Before proving an error estimate between the solutions to problems 2 and 3, we give an estimate for $I_h \tilde{G} - \tilde{I}_h \tilde{G}$ in the $H_{-1}^1(\Omega)$ -norm which will be used in the sequel. With this aim we consider the following auxiliary result.

Lemma 4 *If $G \in \tilde{H}_1^2(\Omega)$ then $\tilde{G} := rG \in H^2(\Omega)$. Moreover, for all $T \in \mathcal{T}_h$*

$$|\tilde{G}|_{H^2(T)}^2 \leq 5r_{\max}^T \|G\|_{\tilde{H}_1^2(T)}^2 + 2 \max\{r^{1-2\varepsilon} : (r, z) \in T\} \|r^{-1} \partial_r(rG)\|_{L_{-1+2\varepsilon}^2(T)}^2 \quad (14)$$

for all $\varepsilon > 0$.

Proof Let $G \in \tilde{H}_1^2(\Omega)$, from (8) it follows that $\tilde{G} := rG \in H_{-1}^1(\Omega) \subset H^1(\Omega)$, thus we focus on the H^2 semi-norm of \tilde{G} , namely, we will show that $\partial_{zz}\tilde{G}$, $\partial_{zr}\tilde{G}$ and $\partial_{rr}\tilde{G}$ belong to $L^2(\Omega)$. Clearly $\partial_{zz}\tilde{G} = r\partial_{zz}G \in L_{-1}^2(\Omega)$. On the other hand, since $r^{-1}\partial_r\tilde{G} = r^{-1}\partial_r(rG)$ belongs to $H_1^1(\Omega)$ (cf. (7)), then $r\partial_z(r^{-1}\partial_r\tilde{G})$, $r\partial_r(r^{-1}\partial_r\tilde{G}) \in L_{-1}^2(\Omega)$ and $r^{-1}\partial_r\tilde{G} \in L^2(\Omega)$, where the last inclusion follows from the continuous embedding $H_1^1(\Omega) \hookrightarrow L^2(\Omega)$ (see Remark 1). Hence, $\partial_{zr}\tilde{G} = r\partial_z(r^{-1}\partial_r\tilde{G}) \in L_{-1}^2(\Omega)$,

$$\partial_{rr}\tilde{G} = \partial_r r(r^{-1}\partial_r\tilde{G}) = r^{-1}\partial_r\tilde{G} + r\partial_r(r^{-1}\partial_r\tilde{G}) \in L^2(\Omega)$$

and thus $\tilde{G} \in H^2(\Omega)$. Let $T \in \mathcal{T}_h$, in order to prove (14) we bound each term on the right-hand side of

$$|\tilde{G}|_{H^2(T)}^2 = \|\partial_{rr}\tilde{G}\|_{L^2(T)}^2 + 2\|\partial_{zr}\tilde{G}\|_{L^2(T)}^2 + \|\partial_{zz}\tilde{G}\|_{L^2(T)}^2. \quad (15)$$

From the previous equalities it is straightforward to obtain that

$$\|\partial_{zz}\tilde{G}\|_{L^2(T)}^2 \leq r_{\max}^T \|\partial_{zz}G\|_{L_1^2(T)}^2, \quad \|\partial_{zr}\tilde{G}\|_{L^2(T)}^2 \leq r_{\max}^T \|\partial_z(r^{-1}\partial_r(rG))\|_{L_1^2(T)}^2$$

and

$$\begin{aligned} \|\partial_{rr}\tilde{G}\|_{L^2(T)}^2 &\leq 2r_{\max}^T \int_T r |\partial_r(r^{-1}\partial_r(rG))|^2 \\ &\quad + 2 \max\{r^{1-2\varepsilon} : (r, z) \in T\} \int_T \frac{1}{r^{1-2\varepsilon}} |r^{-1}\partial_r(rG)|^2 \\ &\leq 2r_{\max}^T \|\partial_r(r^{-1}\partial_r(rG))\|_{L_1^2(T)}^2 \\ &\quad + 2 \max\{r^{1-2\varepsilon} : (r, z) \in T\} \|r^{-1}\partial_r(rG)\|_{L_{-1+2\varepsilon}^2(T)}^2 \end{aligned}$$

for all $\varepsilon > 0$. Thus, from the previous estimates and (15) we obtain

$$\|\tilde{G}\|_{\mathbb{H}^2(T)}^2 \leq 5r_{\max}^T \|G\|_{\mathbb{H}_1^2(T)}^2 + 2 \max\{r^{1-2\varepsilon} : (r, z) \in T\} \|r^{-1}\partial_r(rG)\|_{L_{-1+2\varepsilon}^2(T)}^2$$

which concludes the proof. \square

Lemma 5 For all $\tilde{G} \in \mathbb{H}_{-1}^1(\Omega)$

$$\lim_{h \rightarrow 0} \|I_h \tilde{G} - \tilde{I}_h \tilde{G}\|_{\mathbb{H}_{-1}^1(\Omega^1)} = 0. \quad (16)$$

Additionally, if $r^{-1}\tilde{G} \in \tilde{\mathbb{H}}_1^2(\Omega)$, then for all $\varepsilon > 0$

$$\|I_h \tilde{G} - \tilde{I}_h \tilde{G}\|_{\mathbb{H}_{-1}^1(\Omega^1)} \leq Ch^{1-\varepsilon} \|r^{-1}\tilde{G}\|_{\tilde{\mathbb{H}}_1^2(\Omega)}. \quad (17)$$

Finally, if $\tilde{G} \in \mathbb{H}_{-1}^2(\Omega)$, then

$$\|I_h \tilde{G} - \tilde{I}_h \tilde{G}\|_{\mathbb{H}_{-1}^1(\Omega^1)} \leq Ch \|\tilde{G}\|_{\mathbb{H}_{-1}^2(\Omega)}. \quad (18)$$

Proof Let $\{\phi_j\}_{j=1}^M$ be the nodal basis of \mathcal{L}_h^0 and $\{\mathbf{x}_j\}_{j=1}^M$ be the vertices of the triangulation such that $\phi_j(\mathbf{x}_i) = \delta_{ij}$ for $i, j = 1, \dots, M$. We order these basis functions so that the first M_1 of them correspond to nodal values on the boundary γ_h . From the definition of I_h and \tilde{I}_h it follows that

$$I_h \tilde{G} - \tilde{I}_h \tilde{G} = \sum_{i=1}^{M_1} (I_h \tilde{G})(\mathbf{x}_i) \phi_i \quad \text{in } \Omega_h^1,$$

It is straightforward to show that the basis functions are bounded as follows

$$\|\phi_i\|_{L_{-1}^2(\Omega_h^1 \cap \omega_i)} \leq Ch^{1/2} \quad \text{and} \quad \|\nabla \phi_i\|_{L_{-1}^2(\Omega_h^1 \cap \omega_i)} \leq Ch^{-1/2} \quad i = 1, \dots, M_1,$$

where $\omega_i := \text{supp}(\phi_i)$ and constant C only depends on the regularity of the meshes. From the previous equations we obtain

$$\begin{aligned}
\|I_h \tilde{G} - \tilde{I}_h \tilde{G}\|_{\mathbb{H}_{-1}^1(\Omega^1)}^2 &= \left\| \sum_{i=1}^{M_1} (I_h \tilde{G})(\mathbf{x}_i) \phi_i \right\|_{\mathbb{L}_{-1}^2(\Omega_h^1)}^2 + \left\| \sum_{i=1}^{M_1} (I_h \tilde{G})(\mathbf{x}_i) \nabla \phi_i \right\|_{\mathbb{L}_{-1}^2(\Omega_h^1)}^2 \\
&\leq C \sum_{i=1}^{M_1} |(I_h \tilde{G})(\mathbf{x}_i)|^2 \|\phi_i\|_{\mathbb{L}_{-1}^2(\Omega_h^1 \cap \omega_i)}^2 \\
&\quad + C \sum_{i=1}^{M_1} |(I_h \tilde{G})(\mathbf{x}_i)|^2 \|\nabla \phi_i\|_{\mathbb{L}_{-1}^2(\Omega_h^1 \cap \omega_i)}^2 \\
&\leq Ch^{-1} \sum_{i=1}^{M_1} |(I_h \tilde{G})(\mathbf{x}_i)|^2. \tag{19}
\end{aligned}$$

Next, we bound the last term on the right-hand side of the previous equation. Let $T_i \in \mathcal{T}_h^0$ be such that \mathbf{x}_i is a vertex of T_i , $i = 1, \dots, M_1$ (see Fig. 4 (right)), by proceeding as in [23, Theorem 3.1] it can be prove that

$$|(I_h \tilde{G})(\mathbf{x}_i)| \leq C \|\nabla \tilde{G}\|_{\mathbb{L}^2(\omega_{T_i})}. \tag{20}$$

Let us define $\Omega_h := \cup_{i=1}^{M_1} \text{supp}(\omega_{T_i})$ (see Fig. 4 (right)) then, from (19) and (20) it follows that

$$\begin{aligned}
\|I_h \tilde{G} - \tilde{I}_h \tilde{G}\|_{\mathbb{H}_{-1}^1(\Omega^1)}^2 &\leq Ch^{-1} \sum_{i=1}^{M_1} \|\nabla \tilde{G}\|_{\mathbb{L}^2(\omega_{T_i})}^2 \\
&\leq Ch^{-1} \sum_{i=1}^{M_1} \int_{\omega_{T_i}} \frac{r}{r} |\nabla \tilde{G}|^2 \leq C \|\nabla \tilde{G}\|_{\mathbb{L}_{-1}^2(\Omega_h)}^2.
\end{aligned}$$

Since $\tilde{G} \in \mathbb{H}_{-1}^1(\Omega)$, (16) follows from the previous estimate and Lebesgue's dominated convergence theorem.

Let \tilde{G} be such that $r^{-1} \tilde{G} \in \tilde{\mathbb{H}}_1^2(\Omega)$. To prove (17) we first notice that each component of $\nabla \tilde{G}$ belongs to $\tilde{\mathbb{H}}_1^1(\Omega)$ and thus vanishes on Γ_D . In fact, from (7) it follows that $r^{-1} \tilde{G}, \partial_z(r^{-1} \tilde{G}) \in \tilde{\mathbb{H}}_1^1(\Omega)$ and $\partial_r(r^{-1} \tilde{G}) \in \mathbb{H}_1^1(\Omega)$, then the result is a consequence of the identity $\nabla \tilde{G} = (r \partial_r(r^{-1} \tilde{G}) + r^{-1} \tilde{G}, r \partial_z(r^{-1} \tilde{G}))^\top$. Hence, since $\omega_{T_i} \cap \Gamma_D$ is an edge or union of edges, from (19), (20) and by using the Poincaré inequality it follows that

$$\|I_h \tilde{G} - \tilde{I}_h \tilde{G}\|_{\mathbb{H}_{-1}^1(\Omega^1)}^2 \leq Ch^{-1} \sum_{i=1}^{M_1} \|\nabla \tilde{G}\|_{\mathbb{L}^2(\omega_{T_i})}^2 \leq Ch \sum_{i=1}^{M_1} |\tilde{G}|_{\mathbb{H}^2(\omega_{T_i})}^2. \tag{21}$$

Moreover, by applying Lemma 4 and Remark 1 to estimate the last term of the previous equation we obtain

$$\begin{aligned}
\sum_{i=1}^{M_1} |\tilde{G}|_{\mathbb{H}^2(\omega_{T_i})}^2 &\leq C \sum_{i=1}^{M_1} \left(h \|r^{-1} \tilde{G}\|_{\tilde{\mathbb{H}}_r^2(\omega_{T_i})}^2 + h^{1-2\varepsilon} \|r^{-1} \partial_r \tilde{G}\|_{\mathbb{L}_{-1+2\varepsilon}^2(\omega_{T_i})}^2 \right) \\
&\leq Ch^{1-2\varepsilon} \|r^{-1} \tilde{G}\|_{\tilde{\mathbb{H}}^2(\Omega)}^2 \tag{22}
\end{aligned}$$

for all $\varepsilon > 0$. Thus (17) follows from (21) and (22). We finish the proof by noticing that (18) follows directly from (21) when $\tilde{G} \in \mathbb{H}_{-1}^2(\Omega)$. \square

Now, we are in a position to write the main result of this paper related to the convergence of the proposed scheme

Theorem 1 *Let \tilde{H} and \tilde{H}_h be the solutions to problems 2 and 3, respectively. Then*

$$\lim_{h \rightarrow 0} \|\tilde{H} - \tilde{H}_h\|_{\mathbf{H}^1(\Omega)} = 0. \quad (23)$$

Additionally, let $H_\theta = r^{-1}\tilde{H}$ be the solution of Problem 1. If $H_\theta \in \tilde{\mathbf{H}}_1^2(\Omega)$, then for all $\varepsilon > 0$

$$\|\tilde{H} - \tilde{H}_h\|_{\mathbf{H}^1(\Omega)} \leq Ch^{1-\varepsilon} \|H_\theta\|_{\tilde{\mathbf{H}}_1^2(\Omega)}. \quad (24)$$

Finally, if $rH_\theta \in \mathbf{H}^2(\Omega)$, then

$$\|\tilde{H} - \tilde{H}_h\|_{\mathbf{H}^1(\Omega)} \leq Ch \|rH_\theta\|_{\mathbf{H}^2(\Omega)}. \quad (25)$$

Proof Let \tilde{H} and \tilde{H}_h be the solutions to problems 2 and 3, we note that

$$a(\tilde{H} - \tilde{H}_h, \tilde{H} - \tilde{H}_h) = a(\tilde{H} - \tilde{H}_h, \tilde{H} - \tilde{G}_h) \quad \forall \tilde{G}_h \in \mathcal{X}_h(\mathbf{I}),$$

and, since there exists $C > 0$ such that $C\|\tilde{H} - \tilde{H}_h\|_{\mathbf{H}^1(\Omega)}^2 \leq |a(\tilde{H} - \tilde{H}_h, \tilde{H} - \tilde{H}_h)|$ we have

$$\|\tilde{H} - \tilde{H}_h\|_{\mathbf{H}^1(\Omega)} \leq C\|\tilde{H} - \tilde{G}_h\|_{\mathbf{H}^1(\Omega)} \quad \forall \tilde{G}_h \in \mathcal{X}_h(\mathbf{I}).$$

We notice that $\tilde{H} \in \mathbf{H}^1(\Omega) \subset \mathbf{H}^1(\Omega)$ and thus $\tilde{I}_h\tilde{H}$ is well defined. Moreover, since $\tilde{H} \in \mathcal{X}(\mathbf{I})$ then $I_h\tilde{H}|_{\Gamma_N^k} = \tilde{H}|_{\Gamma_N^k} = \text{constant}$, $k = 0, \dots, N$ and $\tilde{I}_h\tilde{H} \in \mathcal{X}_h(\mathbf{I})$.

Therefore, from the previous inequality and the definition of \tilde{I}_h we have

$$\begin{aligned} \|\tilde{H} - \tilde{H}_h\|_{\mathbf{H}^1(\Omega)} &\leq \|\tilde{H} - \tilde{I}_h\tilde{H}\|_{\mathbf{H}^1(\Omega)} \\ &\leq \|\tilde{H}\|_{\mathbf{H}^1(\Omega^0)} + \|I_h\tilde{H} - \tilde{I}_h\tilde{H}\|_{\mathbf{H}^1(\Omega^1)} + \|\tilde{H} - I_h\tilde{H}\|_{\mathbf{H}^1(\Omega^1)}. \end{aligned} \quad (26)$$

From Lebesgue's dominated convergence theorem and Lemma 5 (cf. (16)) it follows that the first two terms on the right-hand side of the previous equation converge to 0 as $h \rightarrow 0$. To estimate the last term, it is first rewritten as follows

$$\|\tilde{H} - I_h\tilde{H}\|_{\mathbf{H}^1(\Omega^1)}^2 = \|\tilde{H} - I_h\tilde{H}\|_{\mathbf{L}^2(\Omega^1)}^2 + \|\nabla(\tilde{H} - I_h\tilde{H})\|_{\mathbf{L}^2(\Omega^1)}^2 \quad (27)$$

and then we use standard error estimates for the Scott-Zhang interpolant (cf. (12)) to estimate each term

$$\begin{aligned} \|\tilde{H} - I_h\tilde{H}\|_{\mathbf{L}^2(\Omega^1)}^2 &\leq \sum_{T \in \mathcal{T}_h^1} \frac{1}{r_{\min}^T} \int_T |\tilde{H} - I_h\tilde{H}|^2 \\ &\leq \sum_{T \in \mathcal{T}_h^1} \frac{h_T^2}{r_{\min}^T} \int_{\omega_T} |\nabla\tilde{H}|^2 \leq \sum_{T \in \mathcal{T}_h^1} h_T^2 \frac{r_{\max}^T}{r_{\min}^T} \int_{\omega_T} \frac{|\nabla\tilde{H}|^2}{r} \leq Ch^2 \|\tilde{H}\|_{\mathbf{H}^1(\Omega)}^2. \end{aligned} \quad (28)$$

On the other hand, to estimate the semi-norm term in (27) we recall that the set of $\mathcal{C}^\infty(\overline{\Omega})$ functions which vanish in a neighborhood of Γ_D is dense in $\tilde{\mathbf{H}}_1^1(\Omega)$ (see [13, Lemma 3.1]). Then, since $r^{-1}\tilde{H}$ belongs to $\tilde{\mathbf{H}}_1^1(\Omega)$ (cf. (8)), it follows that there exists $\{G_n\}_{n \in \mathbb{N}} \subset \mathcal{C}^\infty(\overline{\Omega})$ such that $G_n \rightarrow r^{-1}\tilde{H}$ in $\tilde{\mathbf{H}}_1^1(\Omega)$. Moreover,

by defining $\tilde{G}_n := rG_n$, it is straightforward to show that $\|\tilde{G}_n - \tilde{H}\|_{\mathbf{H}_{-1}^1(\Omega)} \leq \sqrt{2}\|G_n - r^{-1}\tilde{H}\|_{\tilde{\mathbf{H}}_1^1(\Omega)}$, and hence $\tilde{G}_n \rightarrow \tilde{H}$ in $\mathbf{H}_{-1}^1(\Omega)$. Thus we write

$$\begin{aligned} \tilde{H} - I_h\tilde{H} &= \tilde{H} - (\tilde{G}_n - I_h\tilde{G}_n) - I_h\tilde{H} + (\tilde{G}_n - I_h\tilde{G}_n) \\ &= (\tilde{G}_n - I_h\tilde{G}_n) + (\tilde{H} - \tilde{G}_n) - I_h(\tilde{H} - \tilde{G}_n) \end{aligned}$$

and therefore

$$\begin{aligned} \|\nabla(\tilde{H} - I_h\tilde{H})\|_{\mathbf{L}_{-1}^2(\Omega^1)}^2 &\leq \|\nabla(\tilde{G}_n - I_h\tilde{G}_n)\|_{\mathbf{L}_{-1}^2(\Omega^1)}^2 + \|\nabla((\tilde{H} - \tilde{G}_n) - I_h(\tilde{H} - \tilde{G}_n))\|_{\mathbf{L}_{-1}^2(\Omega^1)}^2. \end{aligned} \quad (29)$$

To bound the first term on the right-hand side of the previous equation we proceed as in (28)

$$\|\nabla(\tilde{G}_n - I_h\tilde{G}_n)\|_{\mathbf{L}_{-1}^2(\Omega^1)}^2 \leq \sum_{T \in \mathcal{T}_h^1} \frac{1}{r_{\min}^T} \int_T |\nabla(\tilde{G}_n - I_h\tilde{G}_n)|^2 \leq \sum_{T \in \mathcal{T}_h^1} \frac{h_T^2}{r_{\min}^T} |\tilde{G}_n|_{\mathbf{H}^2(\omega_T)}^2. \quad (30)$$

The last term of the previous equation can be estimated by applying Lemma 4 (cf. (14)) and Remark 1

$$\begin{aligned} \|\nabla(\tilde{G}_n - I_h\tilde{G}_n)\|_{\mathbf{L}_{-1}^2(\Omega^1)}^2 &\leq \sum_{T \in \mathcal{T}_h^1} \frac{h_T^2}{r_{\min}^T} \left(5r_{\max}^T \|G_n\|_{\tilde{\mathbf{H}}_1^2(T)}^2 \right. \\ &\quad \left. + 2 \max\{r^{1-2\varepsilon} : (r, z) \in T\} \|r^{-1}\partial_r(rG_n)\|_{\mathbf{L}_{-1+2\varepsilon}^2(T)}^2 \right) \\ &\leq Ch^2 \|G_n\|_{\tilde{\mathbf{H}}_1^2(\Omega)}^2 + h^{2-2\varepsilon} \|r^{-1}\partial_r(rG_n)\|_{\mathbf{L}_{-1+2\varepsilon}^2(\Omega)}^2 \\ &\leq h^{2-2\varepsilon} \|G_n\|_{\tilde{\mathbf{H}}_1^2(\Omega)}^2 \end{aligned} \quad (31)$$

for all $\varepsilon > 0$. On the other hand, we use (12) to bound the last term on (29):

$$\begin{aligned} \|\nabla((\tilde{H} - \tilde{G}_n) - I_h(\tilde{H} - \tilde{G}_n))\|_{\mathbf{L}_{-1}^2(\Omega^1)}^2 &\leq \sum_{T \in \mathcal{T}_h^1} \frac{1}{r_{\min}^T} \int_T |\nabla((\tilde{H} - \tilde{G}_n) - I_h(\tilde{H} - \tilde{G}_n))|^2 \\ &\leq \sum_{T \in \mathcal{T}_h^1} \frac{C}{r_{\min}^T} \int_{\omega_T} |\nabla(\tilde{H} - \tilde{G}_n)|^2 \\ &\leq C \sum_{T \in \mathcal{T}_h^1} \frac{r_{\max}^{\omega_T}}{r_{\min}^T} \int_{\omega_T} \frac{1}{r} |\nabla(\tilde{H} - \tilde{G}_n)|^2 \\ &\leq C \|\nabla(\tilde{H} - \tilde{G}_n)\|_{\mathbf{L}_{-1}^2(\Omega)}^2. \end{aligned} \quad (32)$$

Therefore from (27) and (28)-(32) we obtain

$$\|\tilde{H} - I_h\tilde{H}\|_{\mathbf{H}_{-1}^1(\Omega^1)}^2 \leq C \left(h^2 \|\tilde{H}\|_{\mathbf{H}_{-1}^1(\Omega)} + h^{2-2\varepsilon} \|G_n\|_{\tilde{\mathbf{H}}_1^2(\Omega)}^2 + \|\nabla(\tilde{H} - \tilde{G}_n)\|_{\mathbf{L}_{-1}^2(\Omega)}^2 \right).$$

The prove of (23) follows from the previous inequality and the fact that $\tilde{G}_n \rightarrow \tilde{H}$ in $\mathbf{H}_{-1}^1(\Omega)$.

To prove (24) we proceed as before. Since $\tilde{H} = rH$, $H \in \tilde{\mathbb{H}}_1^2(\Omega)$, by using (27), Lemma 5 (cf. (17)) and by proceeding as in (30)-(31) we get

$$\begin{aligned} \|\tilde{H} - \tilde{H}_h\|_{\mathbb{H}_{-1}^1(\Omega)} &\leq \|\tilde{H}\|_{\mathbb{H}_{-1}^1(\Omega^0)} + \|\tilde{H} - I_h\tilde{H}\|_{\mathbb{H}_{-1}^1(\Omega^1)} + \|I_h\tilde{H} - \tilde{I}_h\tilde{H}\|_{\mathbb{H}_{-1}^1(\Omega^1)} \\ &\leq \|\tilde{H}\|_{\mathbb{H}_{-1}^1(\Omega^0)} + h^{1-\varepsilon}\|H\|_{\tilde{\mathbb{H}}_1^2(\Omega)}, \end{aligned} \quad (33)$$

for all $\varepsilon > 0$. Since $r^{-1}\partial_r(rH) \in \mathbb{H}_1^1(\Omega)$, the first term on the right-hand side of the previous equation can be bounded by applying Remark 1

$$\begin{aligned} \|\tilde{H}\|_{\mathbb{H}_{-1}^1(\Omega^0)}^2 &= \int_{\Omega_h^1} \frac{1}{r} r^2 H^2 + \int_{\Omega_h^1} \frac{1}{r} r^2 |\partial_z H|^2 + \int_{\Omega_h^1} \frac{r^{-2\varepsilon}}{r^{1-2\varepsilon}} \frac{1}{r} |\partial_r(rH)|^2 \\ &\leq Ch^2 \int_{\Omega_h^1} \frac{1}{r} H^2 + Ch^2 \int_{\Omega_h^1} \frac{1}{r} |\partial_z H|^2 + \int_{\Omega_h^1} \frac{r^{2-2\varepsilon}}{r^{1-2\varepsilon}} |r^{-1}\partial_r(rH)|^2 \\ &\leq Ch^2 \|H\|_{\mathbb{L}^2(\Omega)}^2 + Ch^2 \|\partial_z H\|_{\mathbb{L}^2(\Omega)}^2 + Ch^{2-2\varepsilon} \|r^{-1}\partial_r(rH)\|_{\mathbb{L}_{r^{-1+2\varepsilon}}^2(\Omega)}^2 \\ &\leq Ch^{2-2\varepsilon} \|H\|_{\tilde{\mathbb{H}}_1^2(\Omega)}, \end{aligned} \quad (34)$$

for all $\varepsilon > 0$. Therefore (24) follows from (33) and (34). Finally, to prove (37) we estimate each term on the right-hand side of (26). Let $\tilde{H} \in \mathbb{H}_{-1}^2(\Omega)$, we bound the first term by applying a Poincaré-type inequality

$$\|\tilde{H}\|_{\mathbb{H}_{-1}^1(\Omega^0)} \leq Ch \|\tilde{H}\|_{\mathbb{H}_{-1}^2(\Omega)},$$

which follows from the fact that $\tilde{H}, \partial_r\tilde{H}, \partial_z\tilde{H} \in \tilde{\mathbb{H}}_1^1(\Omega)$ and thus vanish on Γ_D . For the second term of (26) we apply (18) whereas the last one can be bounded by proceeding as in (28) and using standard error estimates for the Scott-Zhang interpolant (cf. (12)-(13)):

$$\|I_h\tilde{H} - \tilde{I}_h\tilde{H}\|_{\mathbb{H}_{-1}^1(\Omega^1)} + \|\tilde{H} - I_h\tilde{H}\|_{\mathbb{H}_{-1}^1(\Omega^1)} \leq h \|\tilde{H}\|_{\mathbb{H}_{-1}^2(\Omega)}.$$

Hence (37) is a consequence of (26) and the two previous equations. \square

Finally we derive from Theorem 1 an estimate for the original variable H_θ , namely, the magnetic field.

Corollary 2 *Let H_θ and \tilde{H}_h be the solutions to problems 1 and 3, respectively. Then*

$$\lim_{h \rightarrow 0} \|H_\theta - \tilde{H}_h/r\|_{\tilde{\mathbb{H}}_1^1(\Omega)} = 0. \quad (35)$$

Additionally, if $H_\theta \in \tilde{\mathbb{H}}_1^2(\Omega)$, then for all $\varepsilon > 0$

$$\|H_\theta - \tilde{H}_h/r\|_{\tilde{\mathbb{H}}_1^1(\Omega)} \leq Ch^{1-\varepsilon} \|H_\theta\|_{\tilde{\mathbb{H}}_1^2(\Omega)}. \quad (36)$$

Finally, if $rH_\theta \in \mathbb{H}_{-1}^2(\Omega)$, then

$$\|H_\theta - \tilde{H}_h/r\|_{\tilde{\mathbb{H}}_1^1(\Omega)} \leq Ch \|rH_\theta\|_{\mathbb{H}_{-1}^2(\Omega)}. \quad (37)$$

Proof Since $\tilde{H} = rH_\theta$ is solution to Problem 2, the result follows immediately from Theorem 1 and the inequality (cf. (8))

$$\|H_\theta - \tilde{H}_h/r\|_{\tilde{H}_1^1(\Omega)} = \|(rH_\theta - \tilde{H}_h)/r\|_{\tilde{H}_1^1(\Omega)} \leq \|\tilde{H} - \tilde{H}_h\|_{H_{-1}^1(\Omega)}.$$

□

Thus, \tilde{H}_h/r converges to the magnetic field H_θ in $\tilde{H}_1^1(\Omega)$. Moreover, the rate of convergence coincides with that obtained for the solution of Problem 2, although in a different weighted norm.

4 Numerical results

In this section, we present some numerical results obtained with a Fortran code implemented with the help of a new library developed by our group called ForFEM. The code implements Problem 4 described in the Appendix. First, we report a test with a known analytical solution to check the error estimates proved above. Secondly, we apply the method to an industrial problem which arises in the framework of a preforming technique: electro-upsetting [20,21].

4.1 An example with analytical solution

We have solved the eddy current problem in a cylindrical domain $\hat{\Omega}$ of radius R and height L , which is a bounded section of an infinite cylinder (see Fig. 5).

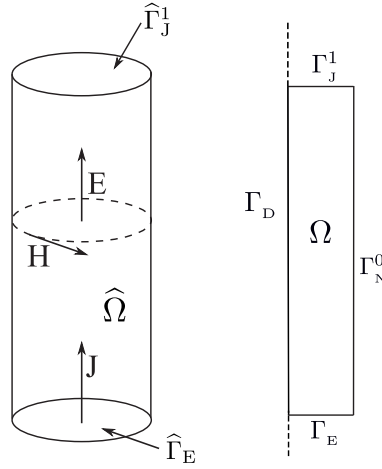


Fig. 5 Sketch of the domain.

We have considered an alternating density \mathbf{J} going through the conductor $\hat{\Omega}$ in the direction of its axis. This current is assumed to be axially symmetric and the current intensity crossing each horizontal section is equal to $I(t) = I_1 \cos(\omega t)$

with I_1 being the amplitude and ω the angular frequency. Thus, we have taken the bottom surface of the cylinder as $\widehat{\Gamma}_E$, its lateral surface as the current density flux-free boundary $\widehat{\Gamma}_N^0$, and its top as $\widehat{\Gamma}_J^1$; see again Fig. 5. Concerning the physical properties, the electric conductivity σ and the magnetic permeability μ have been taken as constants in $\widehat{\Omega}$. Under these assumptions we can obtain an analytical expression for the magnetic field, which only has azimuthal component (see [9] for further details):

$$\begin{aligned}\mathbf{H}(r, \theta, z) &= \frac{I_1}{2\pi R} \frac{\mathcal{I}_1(\gamma r)}{\mathcal{I}_1(\gamma R)} \mathbf{e}_\theta, \\ \mathbf{J}(r, \theta, z) &= \mathbf{curl} \mathbf{H}(r, \theta, z) = \frac{I_1 \gamma}{2\pi R \mathcal{I}_1(\gamma R)} \mathcal{I}_0(\gamma r) \mathbf{e}_z\end{aligned}$$

for all $r \in [0, R]$, $\theta \in [0, 2\pi]$, $z \in [0, L]$, where \mathcal{I}_1 and \mathcal{I}_0 are the modified Bessel functions of the first kind and orders 1 and 0, respectively, and $\gamma := \sqrt{i\omega\mu\sigma} \in \mathbb{C}$.

We have used the following geometrical and physical data:

- $R = 1$ m;
- $L = 1$ m;
- $\sigma = 240000$ (Ωm) $^{-1}$;
- $\mu = \mu_0 = 4\pi \cdot 10^{-7}$ Hm $^{-1}$ (magnetic permeability of free space);
- $I_1 = 62000$ A;
- $\omega = 2\pi \times 50$ Hz.

We have computed the numerical solution of Problem 4 on several successively refined meshes built from a uniform mesh of Ω , a meridional section of $\widehat{\Omega}$; we have compared \widetilde{H}_h with the analytically computed $\widetilde{H} = rH_\theta$ and have also computed the error for the genuine physical variable, namely, the magnetic field. Table 1 shows the percentage errors for both of these quantities and Fig. 6 plots of these errors versus the number of degrees of freedom (d.o.f) in a log-log scale. Notice that the order of convergence for both quantities is clearly $O(h)$, as was predicted by the theoretical results from the previous section.

Table 1 Percentage errors for the computed solution \widetilde{H}_h of Problem 4 in $H_{-1}^1(\Omega)$ -norm and for the magnetic field in $\widetilde{H}_1^1(\Omega)$ -norm.

d.o.f.	$100 \frac{\ \widetilde{H}_h - \widetilde{H}\ _{H_{-1}^1(\Omega)}}{\ \widetilde{H}_h\ _{H_{-1}^1(\Omega)}}$	$100 \frac{\ H_\theta - \frac{\widetilde{H}_h}{r}\ _{\widetilde{H}_1^1(\Omega)}}{\ \frac{\widetilde{H}_h}{r}\ _{\widetilde{H}_1^1(\Omega)}}$
16	60.7647	69.6094
49	29.9278	32.6174
169	14.3020	15.3579
625	7.0384	7.5331
2401	3.5040	3.7478
9409	1.7496	1.8716

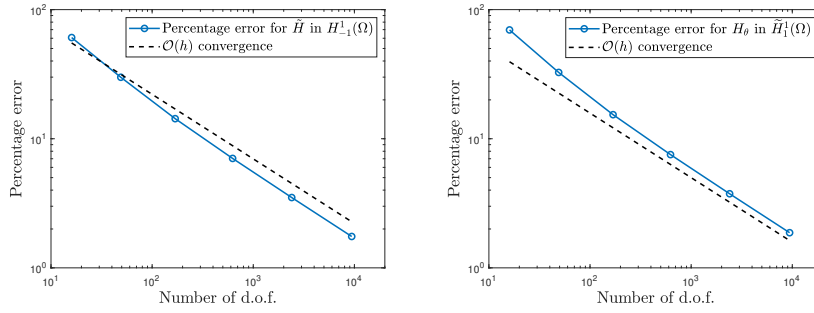


Fig. 6 Percentage errors for the computed solution \tilde{H}_h of Problem 4 in $H^1_{-1}(\Omega)$ -norm (left) and for the magnetic field in $\tilde{H}^1_1(\Omega)$ -norm (right) versus d.o.f (log-log scale).

4.2 Study of the currents in an electro-upsetting application

In this section we report the results obtained by applying the axisymmetric approximation proposed above to compute the current density distribution in a steel cylindrical bar submitted to electric-upsetting.

The process of electric-upsetting consists in passing an electric current through a cylindrical workpiece, which is heated by Joule effect and then deformed to a particular shape. For instance, the process can be used for enlarging the diameter at one of the ends of the piece for later forging in an easier way. In the electric-upsetting process, a cold bar is placed in an horizontal upsetter and clamped by gripper jaws. A low-voltage, high-amperage electric current passes through the bar by contact between one of its ends and the gripper jaws. The currents heats the bar which acquires a plastic behavior. When it reaches enough temperature, the bar is pushed against the anvil with the help of a force applied by an hydraulic cylinder (pusher) located at the opposite end. Thus, the bar enlarges its diameter at the hot end, by getting a shape of onion or ball against the anvil; see Figs. 1 and 7. We notice that electro-upsetting does not provide the finished shape of the manufacturing process, but it provides the preform to be finished by a stamping procedure. Fig. 7 shows a simple sketch and the main elements involved in the process.

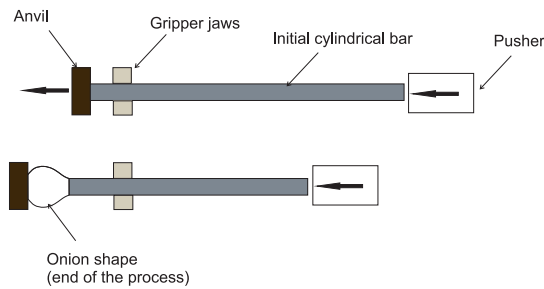


Fig. 7 Sketch of the electro-upsetting process.

In practical cases, the electric current going through the machine can be direct (DC) or alternating (AC). In this example, we consider an alternating current of frequency f and assume that the current intensity crossing the lateral surface of the jaws is known. The potential is fixed to 0 at the end of the anvil.

Although the bar is usually composed of a ferromagnetic material with nonlinear magnetic behavior that also depends on temperature, in this test we assume a linear behavior in order to fit the problem to the analyzed theoretical framework, because our focus here is only in the electromagnetic problem. Let us remark that the formulation could be adapted to a non-linear case, even keeping the harmonic regime to avoid mixing the very different time scales of thermal and electromagnetic problems.

Fig. 8 (left) shows a simple sketch of a cylindrical domain corresponding to the conducting part, which includes the bar, the jaws and the anvil. In its turn, Fig. 8 (right) describes the corresponding meridional section. The electrical ports connected to the source are Γ_J^1 and Γ_E , on the lateral surface of the gripper and the bottom of the anvil, respectively.

We have compared the electromagnetic solution computed by the axisymmetric code with the results of a 3D code implemented in the commercial software Altair Flux.[®] Notice that the 3D simulation requires to build a domain including the conducting part and a dielectric around, in order to impose appropriate approximate boundary conditions. The 3D formulation used by this software is based on the vector electric potential \mathbf{T} and the magnetic scalar potential ϕ (see [19]).

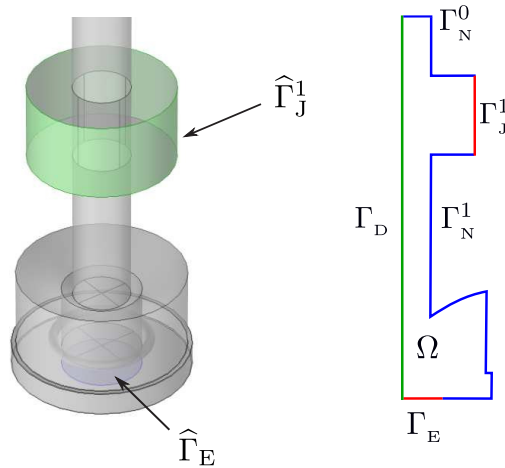


Fig. 8 Sketch of the electro-upsetting process: conducting 3D domain (left) and its meridional section (right).

We have fixed the electrical conductivity of the different materials and compared the results for two different values of the relative magnetic permeability $\mu_r := \mu/\mu_0$ of the bar. In practice, this value changes along the process and consequently the skin effect in the bar is very different at different times.

Fig. 9 shows the modulus of field \tilde{H}_h computed by the 3D (left) and the axisymmetric (right) codes in a meridional section. Notice that the values are very similar, except on the surface corresponding to the current entrance. Let us remark that in our proposed axisymmetric model, the total current crossing this surface is imposed but not the distribution of the current density. Actually, it is not clear whether both codes should lead to similar currents in this part.

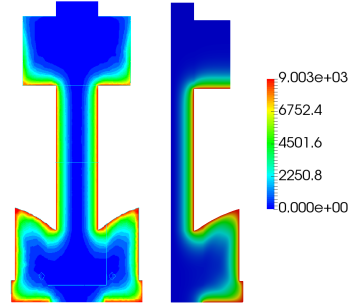


Fig. 9 \tilde{H} field computed with a 3D software (left) and the axisymmetric model (right). Relative magnetic permeability $\mu_r = 10$.

In its turn, Fig. 10 shows the modulus of the current density, which is quite concentrated on the surface of the bar due to the skin effect. Notice that the axisymmetric model is able to capture this effect in an easier way, because finer meshes can be afforded without increasing too much the computational cost. The 3D code would need similarly fine meshes to better capture this effect.

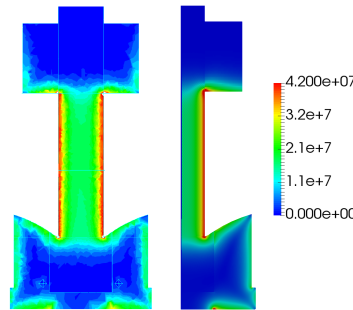


Fig. 10 Current density computed with a 3D software and the axisymmetric model. Relative magnetic permeability $\mu_r = 10$.

This effect can be more clearly observed if we increase the relative magnetic permeability to 100. In such a case, the magnetic field is well approximated (see Figs. 11 and 12), but the skin effect is more diffuse in the 3D case. The latter can be clearly seen by doing a zoom in these figures as that shown on Fig. 12 left.

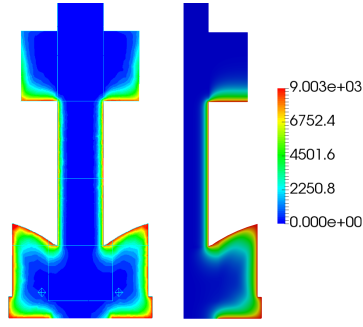


Fig. 11 \tilde{H} field computed with a 3D software and the axisymmetric model. Relative magnetic permeability $\mu_r = 100$.

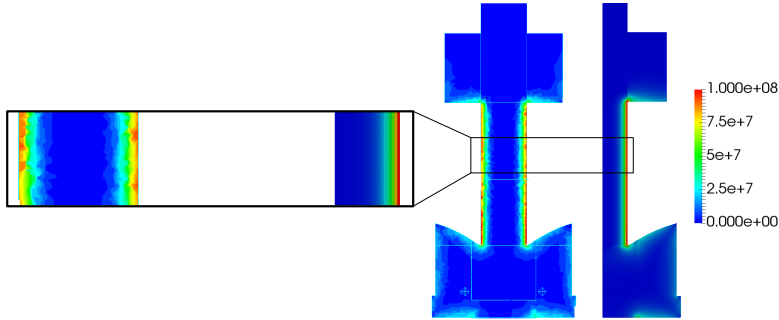


Fig. 12 Current density computed with a 3D software and the axisymmetric model. Relative magnetic permeability $\mu_r = 100$.

A Appendix. A mixed formulation

For the implementation of Problem 3, it is necessary to impose the boundary condition $\tilde{G}_h^k = \tilde{G}_h^{k-1} + \frac{I_k}{2\pi}$, $k \in N_I$. This can be easily obtained by a static condensation procedure applied to the matrix arising from the sesquilinear form $a(\cdot, \cdot)$. However, depending on the computational tool, this boundary constraint can be difficult to implement. In order to propose an alternative for the computational implementation, in this appendix we introduce a mixed finite element approximation of Problem 3 which avoids static condensation. This new formulation could be solved, for instance, by using general purpose finite element software packages like FEniCS [17] and FreeFEM [15].

To begin with, let us introduce a finite element space. Let \mathcal{E} be the set of edges in \mathcal{T}_h lying on Γ_N . Let $e_h^1 \in \mathcal{E}$ be the unique edge of Γ_N^0 intersecting Γ_D (see Fig. 13).

We define

$$\mathcal{P}_h := \{\xi_h \in L^2(\Gamma_N) : \xi_h = 0 \text{ in } e_h^1, \xi_h|_e \in \mathbb{P}_0(e), \forall e \in \mathcal{E}\}.$$

A mixed Galerkin approximation of Problem 2 reads as follows:

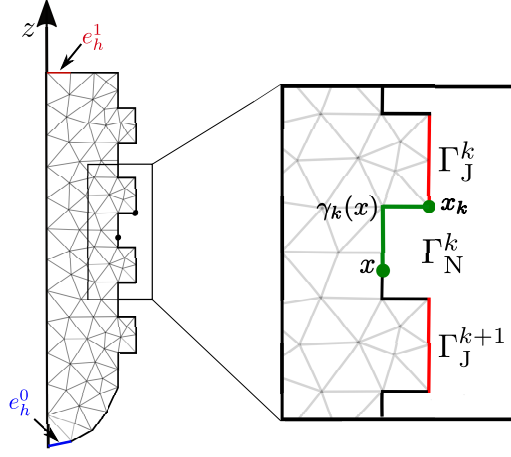


Fig. 13 Notations used in the proof of Lemma 2.

Problem 4 Find $\tilde{H}_h \in \mathcal{Y}_h$, $V_h \in \mathcal{P}_h$ and $V_k \in \mathbb{C}$, $k \in N_I$ such that

$$\begin{aligned} a(\tilde{H}_h, \tilde{G}_h) + \sum_{k=0}^N \int_{\Gamma_N^k} V_h \frac{\partial \tilde{G}_h}{\partial \tau} + \sum_{k \in N_I} \int_{\Gamma_J^k} V_k \frac{\partial \tilde{G}_h}{\partial \tau} &= - \sum_{k \in N_V} V_k (\tilde{G}_h^k - \tilde{G}_h^{k-1}) \\ \sum_{k=0}^N \int_{\Gamma_N^k} \frac{\partial \tilde{H}_h}{\partial \tau} \tilde{\xi}_h &= 0 \\ \sum_{k \in N_I} \int_{\Gamma_J^k} \frac{\partial \tilde{H}_h}{\partial \tau} \bar{W}_k &= \sum_{k \in N_I} \frac{I_k}{2\pi} \bar{W}_k \end{aligned}$$

for all $(\tilde{G}_h, \tilde{\xi}_h, W_k) \in \mathcal{Y}_h \times \mathcal{P}_h \times \mathbb{C}$, $k \in N_I$.

Since $\mathcal{X}_h(\mathbf{0}) \subset \mathcal{Y}_h$ and $\int_{\Gamma_J^k} \frac{\partial \tilde{H}_h}{\partial \tau} = \tilde{H}_h^k - \tilde{H}_h^{k-1}$, it is straightforward to show that if \tilde{H}_h is solution to Problem 4 then is also a solution to Problem 3. Moreover, from the following theorem we obtain the equivalence between problems 3 and 4.

Theorem 2 *Problem 4 has a unique solution.*

Proof Let $\tilde{H}_h \in \mathcal{Y}_h$, $V_h \in \mathcal{P}_h$ and $V_k \in \mathbb{C}$, $k \in N_I$ be a solution of the corresponding Problem 4 with $V_k = 0$, $k \in N_V$ and $I_k = 0$, $k \in N_I$, that is,

$$\begin{aligned} a(\tilde{H}_h, \tilde{G}_h) + \sum_{k=0}^N \int_{\Gamma_N^k} V_h \frac{\partial \tilde{G}_h}{\partial \tau} + \sum_{k \in N_I} \int_{\Gamma_J^k} V_k \frac{\partial \tilde{G}_h}{\partial \tau} &= 0 \quad \forall \tilde{G}_h \in \mathcal{Y}_h, \\ \sum_{k=0}^N \int_{\Gamma_N^k} \frac{\partial \tilde{H}_h}{\partial \tau} \tilde{\xi}_h &= 0 \quad \forall \tilde{\xi}_h \in \mathcal{P}_h, \\ \sum_{k \in N_I} \int_{\Gamma_J^k} \frac{\partial \tilde{H}_h}{\partial \tau} \bar{W}_k &= 0 \quad \forall W_k \in \mathbb{C}, k \in N_I. \end{aligned}$$

Taking $\tilde{G}_h := \tilde{H}_h$, $\xi_h := V_h$ and $W_k := V_k$, $k \in N_1$, we obtain

$$\begin{aligned} a(\tilde{H}_h, \tilde{H}_h) + \sum_{k=0}^N \int_{\Gamma_N^k} V_h \frac{\partial \tilde{H}_h}{\partial \tau} + \sum_{k \in N_1} \int_{\Gamma_J^k} V_k \frac{\partial \tilde{H}_h}{\partial \tau} &= 0, \\ \sum_{k=0}^N \int_{\Gamma_N^k} \frac{\partial \tilde{H}_h}{\partial \tau} \bar{V}_h &= 0, \\ \sum_{k \in N_1} \frac{\partial \tilde{H}_h}{\partial \tau} \bar{V}_k &= 0. \end{aligned}$$

Therefore, $a(\tilde{H}_h, \tilde{H}_h) = 0$. We recall that the sesquilinear form $a(\cdot, \cdot)$ is elliptic in $H_{-1}^1(\Omega)$ then $\tilde{H}_h = 0$. Thus, we have

$$\sum_{k=0}^N \int_{\Gamma_N^k} V_h \frac{\partial \tilde{G}_h}{\partial \tau} + \sum_{k \in N_1} \int_{\Gamma_J^k} V_k \frac{\partial \tilde{G}_h}{\partial \tau} = 0 \quad \forall \tilde{G}_h \in \mathcal{Y}_h. \quad (38)$$

By proceeding as in Lemma 3 it is straightforward to show that, for each $k \in N_1$ there exists $\tilde{G}_{k,h} \in \mathcal{Y}_h$ such that

$$\frac{\partial \tilde{G}_{k,h}}{\partial \tau} = \begin{cases} V_k & \text{on } \Gamma_J^k, \\ 0 & \text{on } \partial\Omega \setminus \Gamma_J^k. \end{cases}$$

By taking $\tilde{G}_h = \tilde{G}_{k,h}$ in (38) we get $|\Gamma_J^k| |V_k|^2 = 0$ and then $V_k = 0$, $k \in N_1$. Next, we prove that V_h also vanishes. With this aim, for each $k \in N$, we introduce the curve $\gamma_k(\mathbf{x})$ with end points \mathbf{x}_k and \mathbf{x} and lying in Γ_N^k (see Fig. 13). For any $k \in N$ we define $\tilde{G}_{k,h} \in \mathcal{Y}_h$ such that, on $\Gamma_N \cup \Gamma_J \cup \Gamma_E$, satisfies

$$\tilde{G}_{k,h}(\mathbf{x}) := \begin{cases} 0 & \mathbf{x} \in e_h^0, \quad \mathbf{x} \in \Gamma_J^i, 1 \leq i \leq k, \quad \mathbf{x} \in \Gamma_N^i, 0 \leq i < k, \\ \int_{\gamma_k(\mathbf{x})} V_h & \mathbf{x} \in \Gamma_N^k, \\ \int_{\Gamma_N^k} V_h & \mathbf{x} \in \Gamma_J^i, k < i < N, \quad \mathbf{x} \in \Gamma_N^i, k \leq i < N. \end{cases}$$

On Γ_E we define $\tilde{G}_{k,h}$ as in Remark 1. Then, by taking $\tilde{G}_h = \tilde{G}_{k,h}$ in (38) we get $V_h = 0$ on Γ_N^k , $\forall k \in N$, and thus $V_h = 0$ on Γ_N . \square

Acknowledgements The work of the authors from Universidade de Santiago de Compostela was supported by FEDER, Ministerio de Economía, Industria y Competitividad-AEI research project MTM2017-86459-R, by Xunta de Galicia (Spain) research project GI-1563 ED431C 2017/60. R. Rodríguez was partially supported by CONICYT-Chile through project AFB170001. P. Venegas was partially supported by FONDECYT-Chile project 1211030. B. López-Rodríguez was partially supported by Universidad Nacional de Colombia through Hermes project 52759.

References

1. A. Alonso-Rodríguez and A. Valli. *Eddy Current Approximation of Maxwell Equations: Theory, Algorithms and Applications*. Springer, 2010.
2. A. Bermúdez, J. Bullón, F. Pena, and P. Salgado. A numerical method for transient simulation of metallurgical compound electrodes. *Finite Elem. Anal. Des.*, 39(4):283–299, 2003.
3. A. Bermúdez, D. Gómez, M. Piñeiro, P. Salgado, and P. Venegas. Numerical simulation of magnetization and demagnetization processes. *IEEE T. Magn.*, 53(12):1–6, 2017.

4. A. Bermúdez, D. Gómez, R. Rodríguez, and P. Venegas. Numerical analysis of a transient non-linear axisymmetric eddy current model. *Comput. Math. Appl.*, 70(8):1984–2005, 2015.
5. A. Bermúdez, D. Gómez, and P. Salgado. *Mathematical Models and Numerical Simulation in Electromagnetism*. New York: Springer, 2014.
6. A. Bermúdez, D. Gómez, P. Salgado, R. Rodríguez, and P. Venegas. Numerical solution of a transient nonlinear axisymmetric eddy current model with nonlocal boundary conditions. *Math. Models Methods Appl. Sci.*, 23(13):2495–2521, 2013.
7. A. Bermúdez, R. Muñoz-Sola, and F. Pena. Existence of a solution for a thermoelectric model with several phase changes and a Carathéodory thermal conductivity. *Nonlinear Anal. Real World Appl.*, 14(6):2212–2230, 2013.
8. A. Bermúdez, C. Reales, R. Rodríguez, and P. Salgado. Numerical analysis of a finite-element method for the axisymmetric eddy current model of an induction furnace. *IMA J. Numer. Anal.*, 30(3):654–676, 2010.
9. A. Bermúdez, R. Rodríguez, and P. Salgado. Numerical treatment of realistic boundary conditions for the eddy current problem in an electrode via Lagrange multipliers. *Math. Comp.*, 74(249):123–151, 2005.
10. C. Bernardi, M. Dauge, and Y. Maday. *Spectral methods for axisymmetric domains*, volume 3 of *Series in Applied Mathematics*. Gauthier-Villars, Éditions Scientifiques et Médicales Elsevier, Paris; North-Holland, Amsterdam, 1999.
11. C. Chaboudez, S. Clain, R. Glardon, D. Mari, J. Rappaz, and M. Swierkosz. Numerical modeling in induction heating for axisymmetric geometries. *IEEE T. Magn.*, 33(1):739–745, 1997.
12. D. Copeland and J. Pasciak. A least-squares method for axisymmetric div-curl systems. *Numer. Linear Algebra Appl.*, 13(9):733–752, 2006.
13. J. Gopalakrishnan and J. Pasciak. The convergence of V-cycle multigrid algorithms for axisymmetric Laplace and Maxwell equations. *Math. Comp.*, 75(256):1697–1719, 2006.
14. H. Haddar and Z. Jiang. Axisymmetric eddy current inspection of highly conducting thin layers via asymptotic models. *Inverse Problems*, 31(11):115005, 25pp, 2015.
15. F. Hecht. New development in FreeFem++. *J. Numer. Math.*, 20(3-4):251–265, 2012.
16. Z. Jiang, H. Haddar, A. Lechleiter, and M. El-Guedri. Identification of magnetic deposits in 2-D axisymmetric eddy current models via shape optimization. *Inverse Probl. Sci. Eng.*, 24(8):1385–1410, 2016.
17. A. Logg, K.-A. Mardal, and G. N. Wells, editors. *Automated solution of differential equations by the finite element method. The FEniCS book*, volume 84 of *Lecture Notes in Computational Science and Engineering*. Springer, Heidelberg, 2012.
18. B. Mercier and G. Raugel. Résolution d’un problème aux limites dans un ouvert axisymétrique par éléments finis en r, z et séries de fourier en θ . *RAIRO, Anal. Numér.*, 16(4):405–461, 1982.
19. G. Meunier, Y. Le Floch, and C. Guerin. A nonlinear circuit coupled $t - t_0 - \phi$ formulation for solid conductors. *IEEE T. Magn.*, 39(3):1729–1732, 2003.
20. P. Nuasri and Y. Aue-u Lan. Investigation of the “surface dimple” defect occurring during the production of an electric upsetting process by viscoplastic finite element modeling. *Int. J. Adv. Manuf. Technol.*, 98(1):1047–1057, 2018.
21. G.-Z. Quan, Z.-Y. Zou, Z.-H. Zhang, and J. Pan. A Study on formation process of secondary upsetting defect in electric upsetting and optimization of processing parameters based on multi-field coupling FEM. *Materials Research*, 19(4):856–864, 2016.
22. J. Querales, R. Rodríguez, and P. Venegas. Numerical approximation of the displacement formulation of the axisymmetric acoustic vibration problem. *SIAM J. Sci. Comput.*, 43:A1583–A1606.
23. L. R. Scott and S. Zhang. Finite element interpolation of nonsmooth functions satisfying boundary conditions. *Math. Comp.*, 54(190):483–493, 1990.
24. R. Touzani and J. Rappaz. *Mathematical models for eddy currents and magnetostatics*. Scientific Computation. Springer, Dordrecht, 2014.
25. R. Van Keer, L.R. Dupré, and J.A.A. Melkebeek. On a numerical method for 2D magnetic field computations in a lamination with enforced total flux. *J. Comp. Appl. Math.*, 72(1):179–191, 1996.

Centro de Investigación en Ingeniería Matemática (CI²MA)

PRE-PUBLICACIONES 2021

- 2021-07 GABRIEL N. GATICA, ANTONIO MARQUEZ, SALIM MEDDAHI: *A virtual marriage a la mode: some recent results on the coupling of VEM and BEM*
- 2021-08 VERONICA ANAYA, RUBEN CARABALLO, BRYAN GOMEZ-VARGAS, DAVID MORA, RICARDO RUIZ-BAIER: *Velocity-vorticity-pressure formulation for the Oseen problem with variable viscosity*
- 2021-09 FELISIA A. CHIARELLO, LUIS M. VILLADA: *On existence of entropy solutions for 1D nonlocal conservation laws with space-discontinuous flux*
- 2021-10 RODOLFO ARAYA, CRISTÓBAL BERTOGLIO, CRISTIAN CÁRCAMO: *Error analysis of pressure reconstruction from discrete velocities*
- 2021-11 GABRIEL N. GATICA, FILANDER A. SEQUEIRA: *An L_p spaces-based mixed virtual element method for the two-dimensional Navier-Stokes equations*
- 2021-12 GABRIEL N. GATICA, CRISTIAN INZUNZA: *On the well-posedness of Banach spaces-based mixed formulations for nearly incompressible elasticity and Stokes models*
- 2021-13 NESTOR SÁNCHEZ, TONATIUH SANCHEZ-VIZUET, MANUEL SOLANO: *Error analysis of an unfitted HDG method for a class of non-linear elliptic problems*
- 2021-14 PAULO AMORIM, RAIMUND BÜRGER, RAFAEL ORDOÑEZ, LUIS M. VILLADA: *Global existence in a food chain model consisting of two competitive preys, one predator and chemotaxis*
- 2021-15 RAIMUND BÜRGER, JULIO CAREAGA, STEFAN DIEHL, ROMEL PINEDA: *A moving-boundary model of reactive settling in wastewater treatment*
- 2021-16 SERGIO CAUCAO, GABRIEL N. GATICA, JUAN P. ORTEGA: *A fully-mixed formulation in Banach spaces for the coupling of the steady Brinkman–Forchheimer and double-diffusion equations*
- 2021-17 DAVID MORA, ALBERTH SILGADO: *A $C1$ virtual element method for the stationary quasi-geostrophic equations of the ocean*
- 2021-18 ALFREDO BERMÚDEZ, BIBIANA LÓPEZ-RODRÍGUEZ, FRANCISCO JOSÉ PENA, RODOLFO RODRÍGUEZ, PILAR SALGADO, PABLO VENEGAS: *Numerical solution of an axisymmetric eddy current model with current and voltage excitations*

Para obtener copias de las Pre-Publicaciones, escribir o llamar a: DIRECTOR, CENTRO DE INVESTIGACIÓN EN INGENIERÍA MATEMÁTICA, UNIVERSIDAD DE CONCEPCIÓN, CASILLA 160-C, CONCEPCIÓN, CHILE, TEL.: 41-2661324, o bien, visitar la página web del centro: <http://www.ci2ma.udec.cl>



**CENTRO DE INVESTIGACIÓN EN
INGENIERÍA MATEMÁTICA (CI²MA)
Universidad de Concepción**



Casilla 160-C, Concepción, Chile
Tel.: 56-41-2661324/2661554/2661316
<http://www.ci2ma.udec.cl>

